Tetrahedron 65 (2009) 2669–2677

Contents lists available at ScienceDirect

Tetrahedron

journal homepage: www.elsevier.com/locate/tet

A new approach toward light-harvesting reverse micelles from donor–acceptor miscible blends

Masaki Takahashi [a,*], Natsuko Nishizawa [a], Shuhei Ohno [a], Masahiro Kakita [a], Norifumi Fujita [b,†], Mitsuji Yamashita [a], Tetsuya Sengoku [a], Hidemi Yoda [a,*]

[a] Department of Materials Science, Faculty of Engineering, Shizuoka University, 3-5-1 Johoku, Naka-ku, Hamamatsu, Shizuoka 432-8561, Japan
[b] Department of Chemistry and Biochemistry, Graduate School of Engineering, Kyushu University, 744 Moto-oka, Nishi-ku, Fukuoka 819-0395, Japan

ARTICLE INFO

Article history:
Received 19 November 2008
Received in revised form 21 January 2009
Accepted 22 January 2009
Available online 30 January 2009

ABSTRACT

In the present paper, we report a new approach toward light-harvesting reverse micellar systems from molecular blends of anthracene and perylene building blocks. The self-assembly initiated by protonation of the molecular blends gave rise to the mixed reverse micelles, in which intermolecular energy transfer from the anthracene to the perylene chromophores was observed. The atomic force microscope (AFM) studies on the reverse micelles prepared from the donor and acceptor blends at a range of the feed ratios showed a number of nanoscale-sized spherical objects homogeneously dispersed on the highly oriented pyrolytic graphite (HOPG) substrate. The critical micelle concentration (cmc) values of the reversed micelles at the donor:acceptor ratios of 100:0, 50:50, and 0:100 were estimated to be 7, 3, and 10 μM by fluorescence batch titrations, respectively, indicating that the cmc values should be almost equivalent regardless of the constitution of each chromophoric component. Attempt to generate the mixed reverse micelles through pairwise mixing of the donor- and acceptor-based reverse micelles resulted in spectral behaviors identical with those obtained by the self-assembly employing the donor–acceptor blends. This suggests that these two reverse micelles undergo thermodynamic exchange of the surfactant molecules to afford the mixed reverse micelles when mixing the two discrete reverse micellar systems.

1. Introduction

The controlled organization of functional dyes into highly ordered self-assembled arrays is an area of research with great potential application in the design of advanced materials such as optoelectronic devices because self-assembly of molecular components through noncovalent interactions is widespread in natural systems.[1] In natural light-harvesting assemblies of photosynthetic bacteria, light-absorbing chromophores are organized in a specific geometry and encapsulated within nanoscopic protein matrices where energy- and electron-transport processes can occur efficiently across photosynthetic membranes.[2] For the development of artificial light-harvesting materials stimulated by the natural photosynthetic systems, confinement of photoactive units within nanoscopic dimensions provides an important strategic advantage in achieving efficient energy transfer directed by the Förster mechanism.[3] From a standpoint of molecular design, reverse micellar aggregates are particularly suited to use as scaffolds in the construction of nanoscale assemblies of antenna pigments due to the fact that the reverse micellar shell provides a unique nanometer-size environment for spatial heterogeneity to bring intermolecular proximity of amphiphilic components.[4] In our previous work, we have studied anthracene–perylene conjugate **1** (Fig. 1), which exhibited efficient light-harvesting functionality arising from intramolecular donor–acceptor interactions, could self-assemble nanoscopic reverse micellar aggregates upon protonation of the tertiary amines (Scheme 1A).[5] As part of our continuing interest in creating light-harvesting reverse micellar systems, the present study focused attention on intermolecular version of energy transfer between donor and acceptor molecules bound in the self-assembled reverse micellar medium (Scheme 1B). The idea of performing energy transfer depending on intermolecular chromophoric interactions in a reverse micellar system led us to synthesize two structurally similar dyes **2** and **3** (Fig. 1), whose anthracene and perylene chromophores fulfill individual roles of the energy donor and acceptor, respectively.[6] When these compounds blended in homogeneous solution are used to generate reverse micellar aggregates through the self-assembly process, the energy donor and acceptor species will be

* Corresponding authors. Tel./fax: +81 53 478 1621/1150.
E-mail addresses: tmtakah@ipc.shizuoka.ac.jp (M. Takahashi), tchyoda@ipc.shizuoka.ac.jp (H. Yoda).
† Present address: Department of Chemistry and Biotechnology School of Engineering, The University of Tokyo, 7-3-1 Hongo, Bunkyo-ku, Tokyo 113-8656, Japan.

0040-4020/$ – see front matter © 2009 Elsevier Ltd. All rights reserved.
doi:10.1016/j.tet.2009.01.089

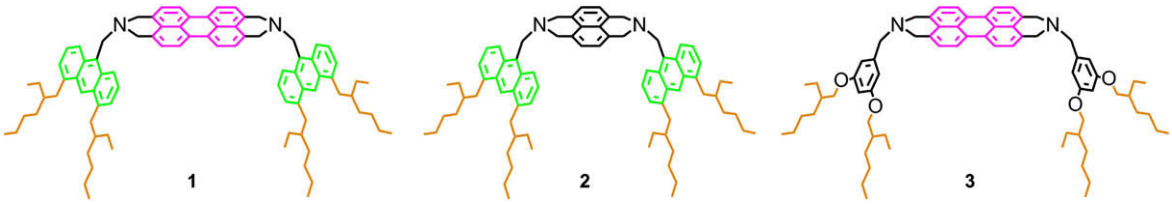

Figure 1. Structures of **1**, **2**, and **3**.

statistically distributed to form the molecular aggregates in heterogeneous (Path A) or homogeneous (Path B) fashion. In the former case (Path A), interactions between the donor and acceptor elements are essentially feasible due to short interchromophore distances that achieve efficient energy transfer, while in the latter (Path B) it is the reverse. In this study, we discovered that the self-assembly of the molecular blends at any feed ratio led to formation of stable reverse micellar aggregates containing both the chromophore elements, in which efficient energy transfer from the donor to the acceptor was observed. Here, we present the details of our studies on the new approach toward the light-harvesting reverse micellar systems from the bichromophoric blends of the two building blocks.

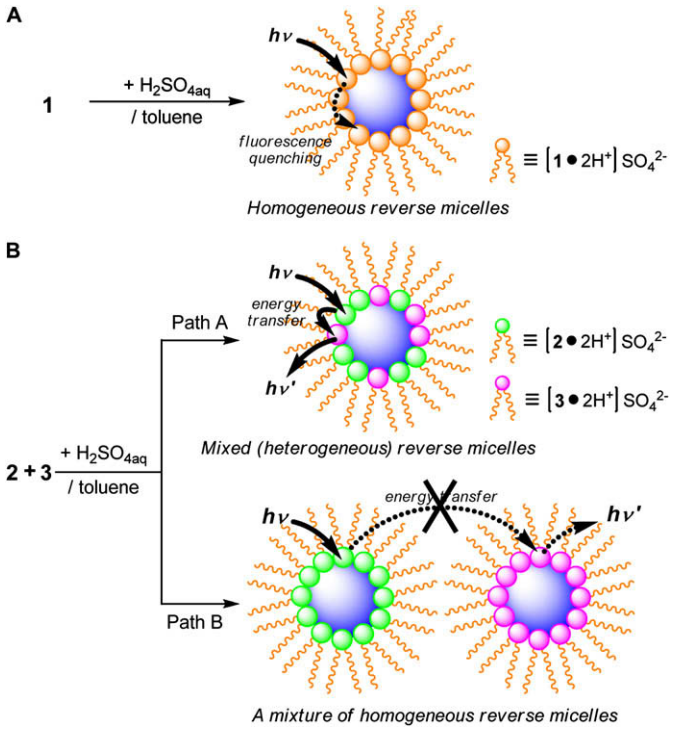

Scheme 1. Schematic representation of the reverse micelle formations.

2. Results and discussion

The two amines **2** and **3**, precursors of the amphiphilic building blocks for creating reverse micelles, were prepared by aluminum hydride reduction of the corresponding naphthalene and perylene bisimides **4** and **5** according to the literature, respectively (Scheme 2).[7] These two key intermediates could be accessed synthetically through condensations of naphthalene and perylene tetracarboxylic dianhydrides (NTCA and PTCA, respectively) with the appropriate amines. While one of the requisite amine, 9-(aminomethyl)-4,5-di(2-ethylhexyl)anthracene, was available from our previous work,[5] the other amine, 1-(aminomethyl)-3,5-di(2-ethylhexyloxy)benzene, was obtained through sequential steps as follows. The preparation of this amine began with Williamson alkylation of commercially available methyl 3,5-dihydroxybenzoate with 2-ethylhexyl bromide to afford **6** in 85% yield. This compound was reduced to the alcohol **7** with lithium aluminum hydride, which was then transformed by treatment with carbon tetrabromide and triphenyl phosphine to give the bromide **8** in 83% for two steps. By employing the Gabriel synthesis, this bromide underwent substitution reaction to form the phthalimide **9**, giving rise to the desired amine **10** (87% for two steps). With these two types of amines in hand, the syntheses of **2** and **3** were accomplished by following the two independent synthetic approaches as described above. These products were fully characterized by elemental analysis and a range of spectroscopies, and further information regarding photophysical properties of the compounds in toluene solutions was obtained by steady-state absorption and fluorescence emission measurements.

In view of the absorption spectra (Fig. 2), **2** exhibited a featureless band attributed to the naphthalene chromophore in the wavelength region around 300 nm as well as three vibrational bands attributed to the anthracene chromophores in the wavelength region from 350 to 410 nm, while **3** displayed a fine structure with two distinct absorption maxima in the wavelength region from 410 to 470 nm, which was assigned to originate from the perylene chromophore. Since the donor (anthracene) and acceptor (perylene) absorptions are well separated in the spectral region, changes of the two populations in the donor–acceptor blends can be monitored by UV–vis absorption spectral measurements. Figure 3A illustrates spectrophotometric titration of the donor–acceptor blends in homogeneous toluene solutions with varying molar ratios of the two components, whose net concentrations were kept constant (c 10.0 μM) throughout the whole surveyed range of the measurements. When changes in absorbance at 341 and 458 nm were plotted as a function of loaded acceptor concentration, linear downward and upward slopes were observed for the donor and acceptor components, respectively (inset of Fig. 3A).

Subsequently, similar experiments were performed by the fluorescence emission measurements on these compounds. Figure 2 also illustrates the fluorescence emission spectra observed upon excitation at 359 nm, exhibiting that the anthracene chromophore of **2** emitted in the wavelength region from 400 to 450 nm, while fluorescence emission from the perylene chromophore of **3** appeared in the wavelength region from 450 to 550 nm. These observations led us to investigate fluorescence emission spectral behavior of the series of donor–acceptor blends in homogeneous toluene solutions. As can be seen in the fluorescence studies (Fig. 3B), the shapes and positions of the donor and acceptor emission bands corresponded apparently to those observed for the two separate components. From the titration plots of the fluorescence intensities at 401 and 494 nm versus the loaded acceptor concentrations (inset of Fig. 3B), we observed trends similar to those found in the absorption behavior, which exhibited two linear dependencies in the concentration region employed. Furthermore, excitation spectra of a series of the donor–acceptor blends at

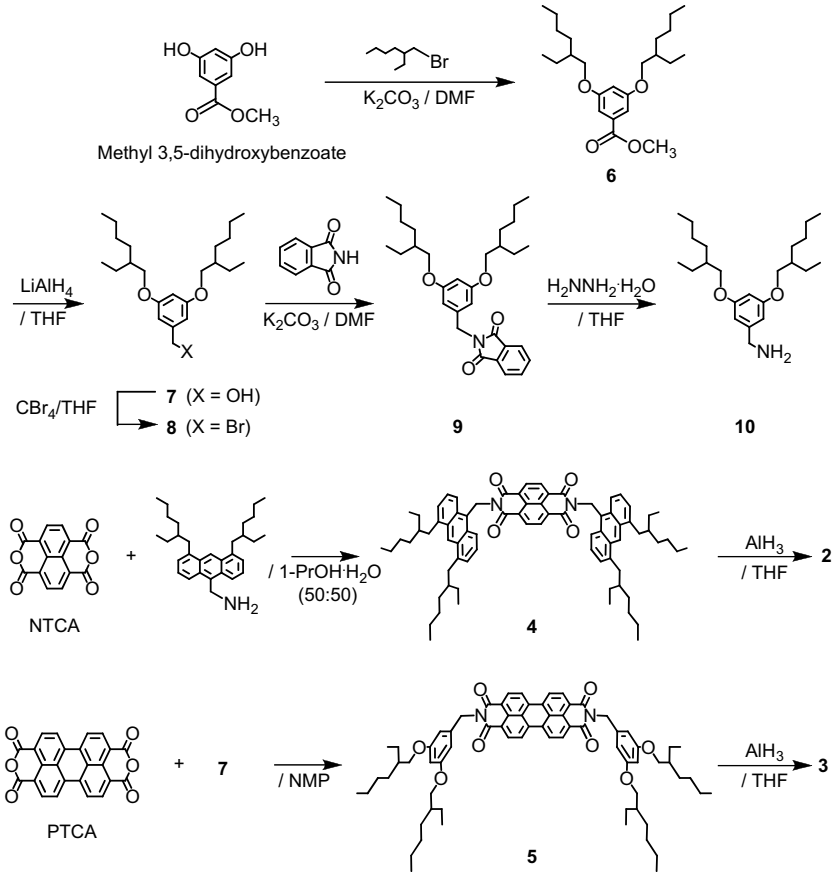

Scheme 2. Preparation of **2** and **3**.

λ_{em} equal to 550 nm exhibited no detectable peaks attributed to the anthracene groups (Fig. 3C). The above results confirm unambiguously that the two chromophores contained in **2** and **3** behave as monomeric species, suggesting that energy transfer promoted by donor–acceptor interactions is unlikely, due to separation distance or relative orientation of the individual molecules dispersed in the highly diluted homogeneous solutions.

On the basis of these observations, we next subjected these compounds to the self-assembly studies. In our previous report, we have established self-assembling approaches with **1** upon protonation of the two tertiary amines at the edges of the perylene core (Scheme 1A). According to the established procedure,[5] an excess (2.0 M equivalents per amines) of sulfuric acid in aqueous solution was added to **2** and/or **3** (0.5 mM in anhydrous toluene) followed by sonication for 3 min and stirring for 18 h at room temperature to promote the self-assembly of the generated surfactants in all of the analytical experiments, in which water/surfactant ratio (W_0) was adjusted to be 50.[8] Figure 4 shows absorption and fluorescence emission spectra of the resulting solutions that were individually prepared from **2** and **3**. In both cases, all absorption maxima observed in both dilute toluene solutions were bathochromically shifted in comparison to the wavelengths of the respective starting compounds, showing notable sign of aggregate formations. Furthermore, significant changes were observed in the fluorescence spectra, which exhibited broad, unstructured, and red-shifted emission bands likely due to excimer-like interacting chromophores within the molecular aggregates in both cases.

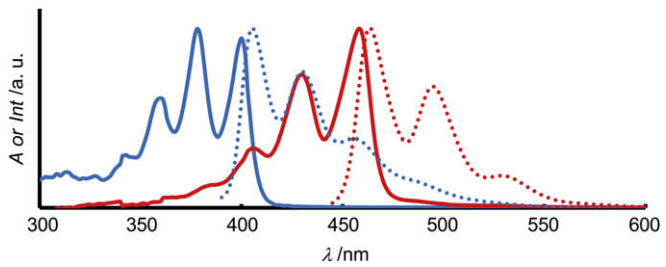

Figure 2. Normalized absorption (solid lines, c 10.0 μM) and fluorescence emission (dotted lines, c 0.1 μM) spectra of **2** (blue lines, λ_{ex}=359 nm), and **3** (red lines, λ_{ex}=430 nm) in toluene.

Since the protonated amines are self-assembled by relatively weak and noncovalent interactions, one must consider the two possible pathways when homogeneous blends of these two structurally similar amines were used for the self-assembly studies (Paths A and B in Scheme 1B). In order to understand fundamental aspects of the self-assembly processes, we set out to explore photophysical behavior of the molecular aggregates formed by the donor–acceptor blends. As can be seen in Figure 5A, the UV–vis spectra in toluene reflected the presence of the donor and acceptor species, whose relative absorbance exhibited linear dependencies on the relevant concentrations. From these observations, the absorption characteristics do not show any pronounced effect related to donor–acceptor interactions between the anthracene and perylene units incorporated within the self-assembled systems.

In contrast, potentially interesting features have emerged when the self-assembled molecular aggregates of the protonated donor–acceptor blends were subjected to the fluorescence measurements (Fig. 5B). Obviously, direct excitation of the energy donor (anthracene) chromophores at 368 nm resulted in pronounced fluorescence

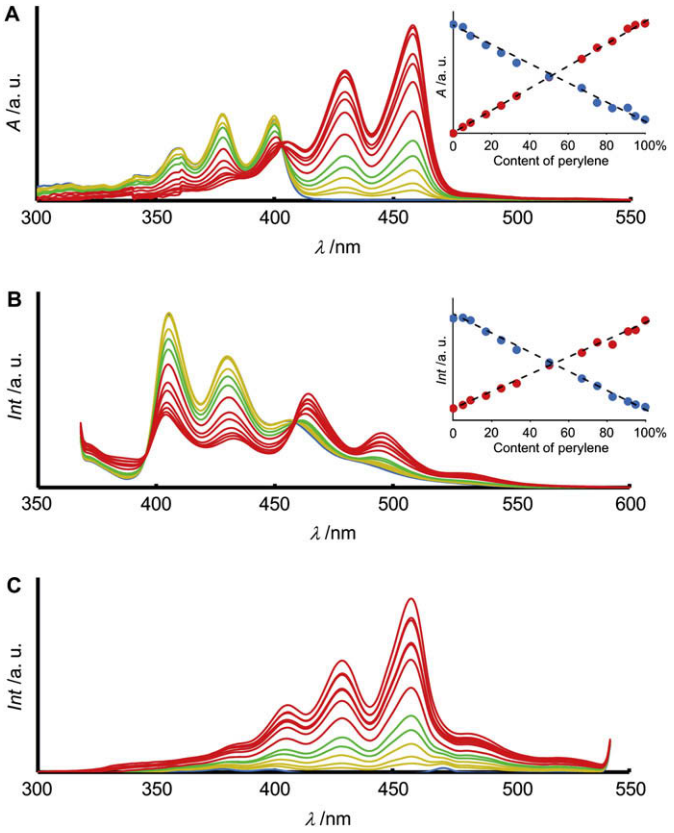

Figure 3. Results of batch spectrophotometric titrations using the donor–acceptor blends at the feed ratios of 100/0, 95/5, 91/9, 83/17, 75/25, 67/33, 50/50, 33/67, 25/75, 17/83, 9/91, 5/95, and 0/100: (A) Absorption spectra (c 10.0 μM) in toluene. Inset: plots of absorbance at 341 nm (blue solid circles) and 458 nm (red solid circles) vs content of the perylene species. (B) Fluorescence emission spectra (λ_{ex}=359 nm, c 0.10 μM) in toluene. Inset: plots of emission intensity at 401 nm (blue solid circles) and 494 nm (red solid circles) vs content of the perylene species. (C) Excitation emission spectra (λ_{em}=550 nm, c 0.10 μM) in toluene.

emission bands from the acceptor (perylene) chromophores in longer-wavelength regions (450–600 nm).[9] It should be noted that the emission maxima for the molecular aggregates are sensitive to the feed ratio of the donor and acceptor components. At low feed ratios (**2**/**3**) greater than 83/17 (orange-colored lines), single emission maxima arising from monomeric perylene acceptor species appeared at 475 nm. By increasing the feed ratio less than 75/25, the fluorescence spectra were red-shifted and less efficient (green-colored lines), leading to suppressed emission from excimer-like perylene aggregates (red-colored lines) in the feed ratios below 50/50. On the basis of these measurements, a reverse micellar model containing the donor–acceptor elements miscible in nanoscopic environments can be proposed to explain the complex photophysical behavior, which

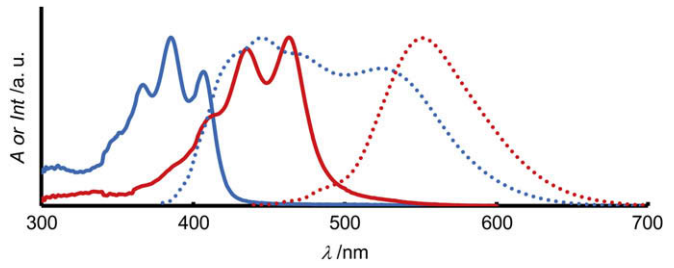

Figure 4. Normalized absorption (solid lines, c 10.0 μM) and fluorescence emission (dotted lines, c 10.0 μM) spectra of the reverse micelles (W_0=50) prepared from **2** (blue lines, λ_{ex}=368 nm) and from **3** (red lines, λ_{ex}=430 nm) in toluene.

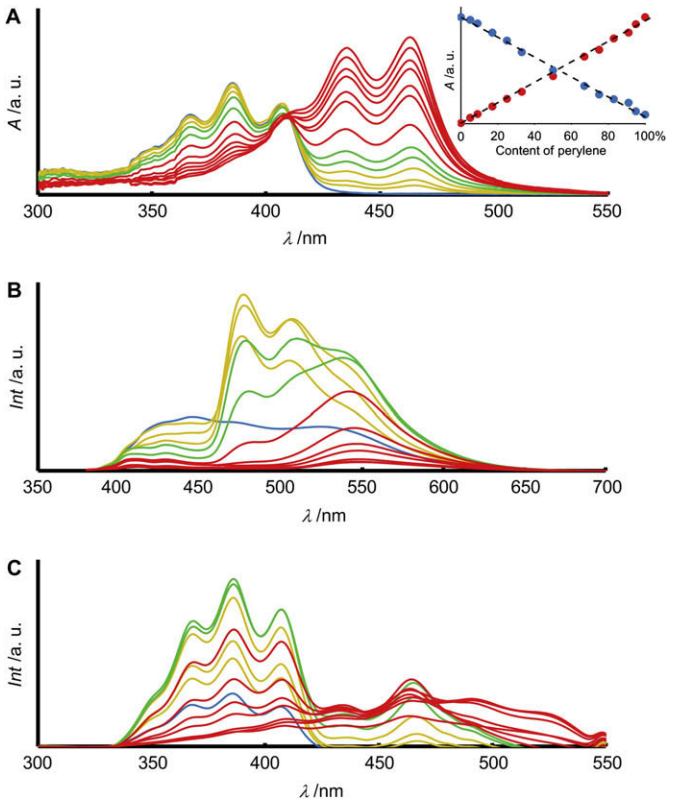

Figure 5. Results of batch spectrophotometric titrations using the reverse micelles (W_0=50) prepared from the donor–acceptor blends at the feed ratios of 100/0, 95/5, 91/9, 83/17, 75/25, 67/33, 50/50, 33/67, 25/75, 17/83, 9/91, 5/95, and 0/100: (A) Absorption spectra of the blends (c 10.0 μM) in toluene. Inset: plots of absorbance at 351 nm (blue solid circles) and 462 nm (red solid circles) vs content of the perylene species. (B) Fluorescence emission spectra (λ_{ex}=368 nm, c 10.0 μM) in toluene. (C) Excitation emission spectra (λ_{em}=550 nm, c 10.0 μM) in toluene.

achieved intermolecular efficient energy transfer from the anthracene donor to the perylene acceptor species.[10]

Another compelling evidence for the energy transfer taking place in the reverse micelles was provided by obtaining the excitation spectra at λ_{em} equal to 550 nm, which corresponds mainly to the acceptor emission (Fig. 5C). Compared with the respective absorption spectra, the excitation spectra are similar in shape, but there are significant differences in the relative intensity ratios of the donor and acceptor signals observed. In fact, the reverse micelles prepared from **2** were found to exhibit three excitation peaks at 368, 386, and 406 nm, which were assigned to excitation region of the anthracene chromophores (blue-colored line). Therefore, we attribute the emission band at 550 nm for a given series of the reverse micelles in part to the broad and red-shifted emission of excimer-like interacting anthracene chromophores. By comparison with the homogeneous reverse micellar systems, the excitation spectral measurements on the mixed reverse micelles prepared from the donor–acceptor blends (e.g., the feed ratio (**2**/**3**)=95/5 or 91/9 or 83/17; orange-colored lines) showed significant enhancement of the three anthracene peaks. The observed enhancement can be ascribed to the 'antenna effect' involving the energy transfer from the anthracene donors to the perylene acceptors.[11] We therefore conclude that the miscible blends of two amines **2** and **3** can self-assemble into the mixed reverse micelles, in which the intermolecular energy transfer is effective as a result of favorable intracluster arrangements of the donor and acceptor chromophores.[12]

Considering the situation where all the chromophoric components are confined within the nanoscopic reverse micellar shells,

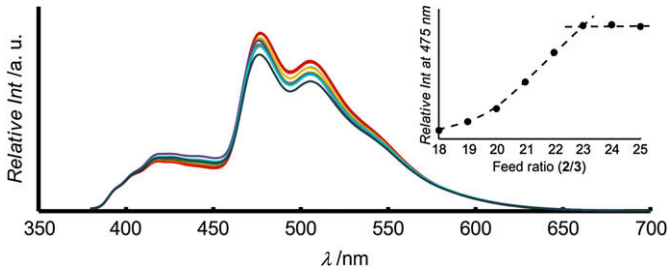

Figure 6. Normalized fluorescence emission spectra (λ_{ex}=368 nm) of the mixed reverse micelles at the feed ratios (**2**/**3**) from 18/1 to 25/1 (c 10.0 μM) with respect to the perylene concentrations. Inset: plots of relative fluorescence intensity at 475 nm vs the feed ratio.

the intracluster energy transfer directed by the Förster mechanism is highly efficient and results in amplification of the acceptor emission upon excitation of the donor chromophores.[13] Thus, the above spectroscopic evidence can be obviously regarded as the proposed reverse micellar system by taking into account the fact that the energy transfer from the anthracene donor to the perylene acceptor occurs with sufficiently high efficiency.[14] Based on this mechanistic model, we deduce that the presence of more than two perylene species within a reverse micelle aggregate causes suppression of the acceptor emissions due to collisional quenching driven by non-negligible interactions among the neighboring acceptors. In other words, a reverse micellar system containing completely isolated perylene species among the anthracene donor clusters leads to the most enhanced acceptor emission. To validate this assumption, the fluorescence spectra were normalized with respect to the donor concentrations and reexamined in the specific range of the feed ratios from 18/1 to 25/1 (Fig. 6). For comparison, the relative intensities of the acceptor emission maxima at 475 nm were plotted in the inset of Figure 6 as a function of the feed ratio (**2**/**3**). This titration plot shows a moderately growing curve that reaches a plateau at the feed ratio of 23. We therefore conclude that one set of the reverse micellar aggregate prepared from **2** is built up of ca. 24 surfactant molecules. Unfortunately, there is no straightforward way to apply this estimation methodology to the reverse micelle prepared from **3**, unless alternative donor surfactant compatible with the perylene chromophore is available.

To explore nanoscopic features of the self-assembled aggregate systems, the atomic force microscope (AFM) studies were carried out on the reverse micelles prepared from the donor and acceptor blends at a range of the feed ratios (**2**/**3**=100/0, 75/25, 67/33, 50/50, 25/75, 33/67, and 0/100). As can be seen in Figure 7, there are a number of small spherical objects dispersed on the highly oriented pyrolytic graphite (HOPG) substrate, which can be attributed to the individual reverse micelles or their assemblies.[15] Throughout inspection of the given series of the AFM pictures, it would appear that acceptor-rich reverse micelles have a tendency to form relatively large spherical objects. At this point, it is reasonable to assume that molecular size of the surfactant components would play a critical role in determining size and shape of the reverse micelles. In terms of structural description of our designed donor and acceptor molecules, considerable size difference can be found in end-to-end lengths of naphthalene (0.68 nm) and perylene (1.11 nm) nuclei, whereas two different 2-ethylhexyl-cont aining side groups are similar in size and shape. With this idea in mind, we can deduce that this structural difference and the composition of the donor–acceptor blends may reflect overall average size of the self-assembled aggregates. Zoomed AFM images and cross-sectional views for the reverse micelles prepared from **2** are shown in Figure 8, revealing that the small spherical objects appeared to have an average height less than 3 nm.[16] These results suggest the reverse micelles are stabilized in the nanoscopic globular forms, where the chromophoric components are in close contact. The formation of these coherent domains may be a consequence of noncovalent interactions between the amphiphilic components, allowing the efficient energy transfer or fluorescence radiationless deactivation due to the concentration quenching.

To determine critical micelle concentration (cmc) values of the reverse micelles, we investigated titrations using various concentrations of the surfactant molecules from 0.5 to 80 μM. As has been observed previously, the cmc values for the homogeneous reverse micellar systems can be defined phenomenologically from changes in the fluorescence output, whose efficiency should decrease steadily in a concentration range close to the cmc as a result of the fluorescence deactivation due to the concentration quenching or

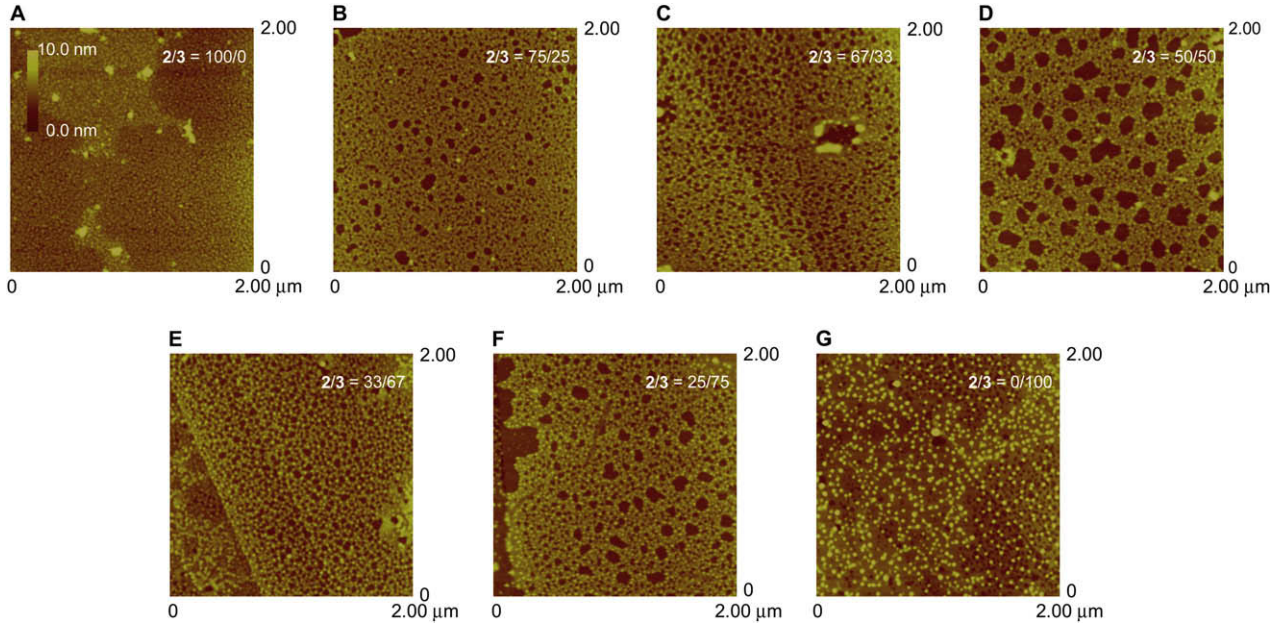

Figure 7. AFM images of drop-cast of the mixed reverse micelles (W_0=50) at the feed ratios of (A) 100/0, (B) 75/25, (C) 67/33, (D) 50/50, (E) 33/67, (F) 25/75, and (G) 0/100.

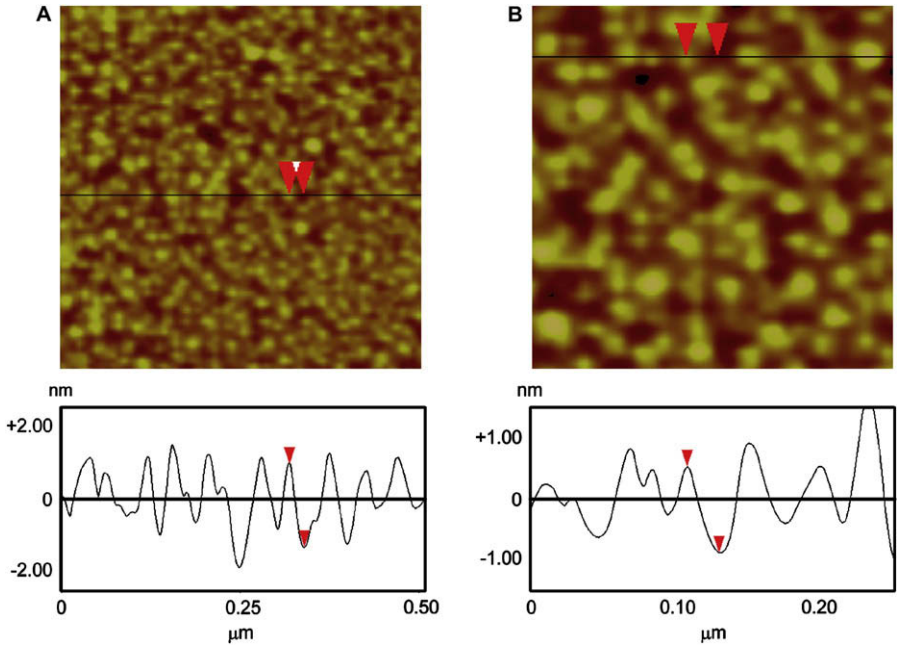

Figure 8. Two types of zoom-in images of Figure 7A; (A) 0.5×0.5 μm and (B) 0.2×0.2 μm (top). The height profiles on cross-sections of the solid lines in the AFM images (bottom).

energy transfer.[17] In the cases of the homogeneous reverse micelles, the titration plots of fluorescence intensities showed linear relationship at lower concentrations and reached a plateau above 40 μM (Fig. 9A and 9B). From a given inflection point in the fluorescence emission trajectory, we estimated the cmc values for the homogeneous reverse micelles prepared from **2** and **3** as 7 and 3 μM, respectively. On the other hand, the cmc values for the mixed reverse micellar systems involving the energy transfer (e.g., the feed ratio=50/50) can be approximated by monitoring consecutively the fluorescence intensity of the donor species. Formation of the mixed reverse micelles leads to introduction of the light-harvesting functionality, resulting in significant decrease of the donor emission upon excitation of the donor chromophores due to the energy transfer. For this reason, the monitoring runs were performed by scanning the fluorescence emission at 405 nm with excitation at 340 nm. Under this condition, the titration plot showed a distinct reflection point at the concentration of 10 μM (Fig. 9C), which corresponds to the cmc value for the mixed reverse micelles. The results from these titration experiments on the three different reverse micellar systems suggest that the cmc values are almost equivalent regardless of the constitution of each chromophoric component.

Alternate approach to the mixed reverse micelles was next explored in order to address a question concerning the feasibility of molecular exchange between two types of the homogeneous reverse micelles (Scheme 3). To test this possibility, we attempted pairwise mixing of the donor- and acceptor-based reverse micelles prepared individually from **2** and **3**, respectively, at the stoichiometric ratios of 10:1, 3:1, and 1:1 (*c* 0.5 mM, at room temperature for 3 min). Formation of the mixed reverse micelles can be confirmed by comparison with control experiment on those prepared from the donor–acceptor blends at the respective feed ratios. Indeed, all the fluorescence spectra obtained from the mixing approaches were found to be identical with those obtained from the control experiments, indicating introduction of the light-harvesting functionality. These spectroscopic observations suggest that these two homogeneous reverse micelles undergo thermodynamic exchange of the surfactant molecules to afford the mixed reverse micelles when mixing the two components. On the basis of these

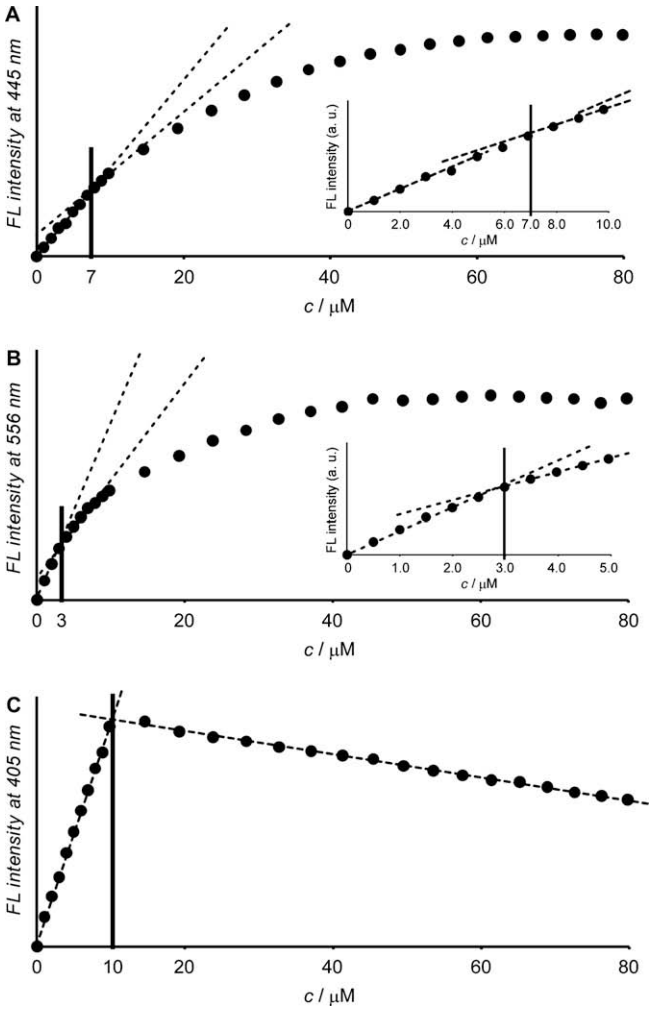

Figure 9. Plots of fluorescence intensities of the reverse micelles prepared from (A) **2** and (B) **3** and (C) donor–acceptor blend at the feed ratio (**2**/**3**) of 50/50 vs concentrations of the analytes.

results, we believe that the dynamic nature of the blending techniques would give many potential applications in generating a dynamic combinatorial library of the light-harvesting reverse micellar systems.[18]

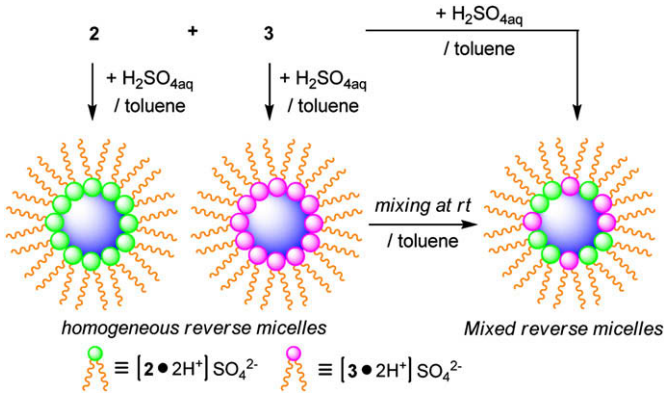

Scheme 3. Schematic representation of pairwise mixing of the donor- and acceptor-based reverse micelles.

3. Conclusions

We have studied a new approach to the self-assembly of the donor–acceptor miscible blends, which spontaneously generated the mixed reverse micelles in nanoscopic dimensions. The interesting finding here is that the mixed reverse micelles achieve intermolecular energy transfer from the anthracene donor to the perylene acceptor, making it possible to introduce the light-harvesting functionality. As a result of the heterogeneous nature, the mixed reverse micellar systems ensure the unique color emission profiles, which can be tuned by adjusting the composition of the donor–acceptor elements. These studies would suggest that our self-assembling approaches to the mixed reverse micelles via the combination of photoactive species may provide a conceptual basis for creating artificial light-harvesting nanostructured materials with diverse and properly designed functionality.[19] Further studies on the development of this self-assembly approaches to novel light-harvesting reverse micellar systems for practical uses and engineering new applications will be the subject of future work.

4. Experimental section

4.1. General

All solvents and reagents were of reagent grade quality from Wako Pure Chemicals and Tokyo Chemical Industry (TCI) used without further purification. The ^{1}H and ^{13}C nuclear magnetic resonance (NMR) spectra operating at the frequencies of 300 and 75 MHz, respectively, were recorded on a JEOL JNM-AL300 spectrometer in chloroform-*d* ($CDCl_3$). Chemical shifts are reported in parts per million (ppm) relative to TMS and the solvent used as internal standards, and the coupling constants are reported in hertz (Hz). Fourier transform infrared (FTIR) spectra were recorded on Shimadzu FTIR-8200A spectrometers. UV–vis and fluorescence (excitation) spectra were recorded on a JASCO V-530 spectrophotometer and a JASCO FP-6200 spectrofluorometer, respectively. Molar absorption coefficients (ε) were determined by batch spectrophotometric titrations. Plots of absorbance of analytes at wavelengths of interest versus relevant concentrations should be linear if the titration studies were performed at sufficient low absorbance ($A<1.0$). The slopes of these linear plots allow the calculation of the molar absorption coefficients for the analytes examined. Matrix-assisted laser desorption ionization time of flight (MALDI-TOF) mass spectra were recorded on an Applied Biosystems Voyager-DE PRO mass spectrometer by carrying out measurements in reflector mode with the matrix 1,8,9-trihydroxy anthracene (dithranol) that were dissolved in THF and mixed with the analytes at a molar ratio of approximately 1:500 (analyte:matrix). High resolution mass spectrometry (HRMS) was performed on a JEOL JMS-T100CS. Elemental analyses were performed by Thermo Flash EA 1112 and JSL Model JM 10 instruments. The atomic force microscope (AFM) analyses were performed on a Veeco NanoScope IIIa microscope.

4.2. Preparation and characterization of new compounds

4.2.1. *Methyl 3,5-di(2-ethylhexyloxy)benzoate (**6**)*

A solution containing methyl 3,5-dihydroxybenzoate (0.100 g, 0.595 mmol), 2-ethylhexyl bromide (0.35 mL, 1.97 mmol), and potassium carbonate (0.168 g, 1.21 mmol) in DMF (1 mL) was heated at 100 °C with stirring under argon atmosphere. After 10 h, the reaction mixture was cooled to room temperature, filtered through a pad of Celite, and then extracted with hexane (30 mL). The organic layer was washed with water (100 mL) and brine (20 mL), dried over anhydrous Na_2SO_4, filtered, and concentrated in vacuo. The residue was purified by silica gel column chromatography (hexane/ethyl acetate=30/1) to give **6** (0.198 g, 85%) as a colorless oil: IR (NaCl) 1173 cm^{-1} (C–O), 1597 cm^{-1} (C=C), 1724 cm^{-1} (C=O); ^{1}H NMR ($CDCl_3$) δ 0.85–0.97 (m, 12H, *Me*), 1.25–1.60 (m, 16H, CH_2), 1.65–1.78 (m, 2H, C*H*), 3.86 (d, J=5.6 Hz, 4H, CH_2), 3.90 (s, 3H, *Me*), 6.65 (t, J=2.2 Hz, 1H, Ar*H*), 7.17 (d, J=2.2 Hz, 2H, Ar*H*); ^{13}C NMR ($CDCl_3$) δ 11.2 (CH_3), 14.1 (CH_3), 23.1 (CH_2), 24.0 (CH_2), 29.2 (CH_2), 30.6 (CH_2), 39.5 (C*H*), 52.2 (CH_3), 70.8 (CH_2), 106.7 (C*H*), 107.8 (C*H*), 132.0 (*C*), 160.7 (*C*), 167.3 (*C*). Anal. Calcd for $C_{24}H_{40}O_4$: C, 73.43; H, 10.27. Found: C, 73.09; H, 10.25.

4.2.2. *3,5-Di(2-ethylhexyloxy)phenyl methanol (**7**)*

To a solution of **6** (1.79 g, 4.56 mmol) in anhydrous THF (10 mL) was added lithium aluminum hydride (0.173 g, 4.56 mmol) in small portions over a period of 20 min at 0 °C. After stirring for 3 h at room temperature, the reaction was quenched by addition of water (5 mL) and 3% aqueous HCl (10 mL) at 0 °C. The resulting reaction mixture was then extracted with hexane (100 mL). The organic layer was washed with water (100 mL), saturated aqueous $NaHCO_3$ (20 mL), and brine (20 mL). The extract was separated, dried over anhydrous Na_2SO_4, filtered, and concentrated in vacuo to give **7** (1.48 g, 89%) as a colorless oil: IR (NaCl) 1171 cm^{-1} (C–O), 1597 cm^{-1} (C=C), 3346 cm^{-1} (O–H); MS (MALDI-TOF) m/z 365.7 (MH^+); ^{1}H NMR ($CDCl_3$) δ 0.85–0.97 (m, 12H, *Me*), 1.25–1.56 (m, 16H, CH_2), 1.61–1.76 (m, 3H, C*H* and O*H*), 3.83 (dd, J=0.8 and 5.7 Hz, 4H, CH_2), 4.62 (d, J=5.9 Hz, 2H, CH_2), 6.39 (t, J=2.2 Hz, 1H, Ar*H*), 6.51 (d, J=2.2 Hz, 2H, Ar*H*); ^{13}C NMR ($CDCl_3$) δ 11.2 (CH_3), 14.1 (CH_3), 23.1 (CH_2), 24.0 (CH_2), 29.2 (CH_2), 30.6 (CH_2), 39.5 (C*H*), 65.3 (CH_2), 70.6 (CH_2), 100.7 (C*H*), 105.2 (C*H*), 143.5 (*C*), 161.0 (*C*). Anal. Calcd for $C_{23}H_{40}O_3$: C, 75.77; H, 11.06. Found: C, 75.96; H, 11.08.

4.2.3. *3,5-Di(2-ethylhexyloxy)phenylmethyl bromide (**8**)*

To a stirring mixture of **7** (1.49 g, 4.08 mmol), carbon tetrabromide (1.76 g, 5.30 mmol), and triphenyl phosphine (1.40 g, 5.30 mmol), was added anhydrous THF (2 mL) at room temperature. After stirring for 1 h at room temperature, hexane (100 mL) was added to the reaction mixture, whereupon the resultant white precipitate was filtered through a pad of Celite under vacuum. The filtrate was washed with water (100 mL) and brine (50 mL), dried over Na_2SO_4, filtered, and concentrated in vacuo. The residue was purified by silica gel column chromatography (hexane/ethyl acetate=30/1) to give **8** (1.62 g, 93%) as a colorless oil: IR (NaCl) 1173 cm^{-1} (C–O), 1597 cm^{-1} (C=C); MS (MALDI-TOF) m/z 427.5 (MH^+); ^{1}H NMR ($CDCl_3$) δ 0.85–0.97 (m, 12H, *Me*), 1.25–1.55 (m,

16H, CH_2), 1.63–1.77 (m, 2H, C*H*), 3.81 (dd, *J*=0.8 and 5.7 Hz, 4H, CH_2), 4.41 (s, 2H, CH_2), 6.39 (t, *J*=2.2 Hz, 1H, Ar*H*), 6.52 (d, *J*=2.2 Hz, 2H, Ar*H*); ^{13}C NMR ($CDCl_3$) δ 11.2 (*C*H_3), 14.1 (*C*H_3), 23.1 (*C*H_2), 23.9 (*C*H_2), 29.1 (*C*H_2), 30.6 (*C*H_2), 33.9 (*C*H_2), 39.5 (*C*H), 70.6 (*C*H_2), 101.6 (*C*H), 107.5 (*C*H), 139.7 (*C*), 160.9 (*C*). Anal. Calcd for $C_{23}H_{39}BrO_2$: C, 64.63; H, 9.20. Found: C, 64.44; H, 9.38.

4.2.4. 3,5-Di(2-ethylhexyloxy)-1-(phthalimidomethyl)benzene (**9**)

A suspension of **8** (0.144 g, 0.337 mmol), phthalimide (0.064 g, 0.438 mmol), and potassium carbonate (0.070 g, 0.506 mmol) in DMF (5 mL) was stirred at room temperature. After stirring for additional 22 h, it was filtered through a pad of Celite under vacuum and washed with ethyl acetate (100 mL). The filtrate was washed with water (100 mL) and brine (50 mL), dried over Na_2SO_4, filtered, and concentrated in vacuo. Purification of the residue by flash column chromatography on silica gel (hexane/ethyl acetate=20/1) gave **9** (0.163 g, 98%) as a colorless oil: IR (NaCl) 1597 cm^{-1} (C=C), 1609 cm^{-1} (C=C), 1717 cm^{-1} (C=O), 1773 cm^{-1} (C=O); MS (MALDI-TOF) *m*/*z* 494.9 (MH^+); ^{1}H NMR ($CDCl_3$) δ 0.85–0.95 (m, 12H, *Me*), 1.24–1.56 (m, 16H, CH_2), 1.61–1.74 (m, 2H, C*H*), 3.80 (d, *J*=5.5 Hz, 4H, CH_2), 4.76 (s, 2H, CH_2), 6.36 (t, *J*=2.2 Hz, 1H, Ar*H*), 6.56 (d, *J*=2.2 Hz, 2H, Ar*H*), 7.69 (dd, *J*=3.0 and 5.5 Hz, 2H, Ar*H*), 7.84 (dd, *J*=3.0 and 5.5 Hz, 2H, Ar*H*); ^{13}C NMR ($CDCl_3$) δ 10.9 (*C*H_3), 13.9 (*C*H_3), 22.9 (*C*H_2), 23.7 (*C*H_2), 28.9 (*C*H_2), 30.4 (*C*H_2), 39.3 (*C*H), 41.6 (*C*H_2), 70.3 (*C*H_2), 100.6 (*C*H), 106.8 (*C*H), 123.3 (*C*H), 132.2 (*C*), 133.9 (*C*H), 138.3 (*C*), 160.8 (*C*), 168.0 (*C*). Anal. Calcd for $C_{31}H_{43}NO_4$: C, 75.42; H, 8.78. Found: C, 75.67; H, 8.94.

4.2.5. 1-(Aminomethyl)-3,5-di(2-ethylhexyloxy)benzene (**10**)

To a solution of **9** (0.257 g, 0.521 mmol) in THF (5 mL) was slowly added hydrazine monohydrate (0.1 mL, 3.15 mmol) at ambient temperature and the resulting reaction mixture was heated at reflux. After 3 h, it was cooled to ambient temperature, filtered through a pad of Celite, and washed with hexane (50 mL). The filtrate was washed with water (50 mL) and brine (20 mL), dried over Na_2SO_4, filtered, and concentrated in vacuo to give **10** (0.168 g, 89%) as a colorless oil; IR (NaCl) 1171 cm^{-1} (C–O), 1595 cm^{-1} (C=C), 3421 and 3377 cm^{-1} (N–H); MS (MALDI-TOF) *m*/*z* 364.9 (MH^+); HRMS (ESI) *m*/*z* calcd for $C_{23}H_{42}NO_2$: 364.3216, found 364.3195; ^{1}H NMR ($CDCl_3$) δ 0.85–0.97 (m, 12H, *Me*), 1.25–1.58 (m, 18H, CH_2 and NH_2), 1.63–1.77 (m, 2H, C*H*), 3.78 (s, 2H, CH_2), 3.82 (d, *J*=5.5 Hz, 4H, CH_2), 6.35 (t, *J*=2.2 Hz, 1H, Ar*H*), 6.45 (d, *J*=2.2 Hz, 2H, Ar*H*); ^{13}C NMR ($CDCl_3$) δ 11.2 (*C*H_3), 14.1 (*C*H_3), 23.1 (*C*H_2), 24.0 (*C*H_2), 29.2 (*C*H_2), 30.7 (*C*H_2), 39.5 (*C*H), 46.8 (*C*H_2), 70.5 (*C*H_2), 99.8 (*C*H), 105.4 (*C*H), 145.9 (*C*), 161.1 (*C*). Anal. Calcd for $C_{23}H_{41}NO_2$: C, 75.98; H, 11.37; N, 3.85. Found: C, 76.10; H, 11.00; N, 4.03.

4.2.6. 2,7-Bis(4,5-di(2-ethylhexyl)-9-anthracenemethyl)-2,7-diazadibenzo[de,ij]naphthalene-1,3,6,8-tetraone (**4**)

To a suspension of naphthalene-1,4,5,8-tetracarboxylic dianhydride (0.0594 g, 0.222 mmol) and 9-(aminomethyl)-4,5-di(2-ethylhexyl)anthracene (0.287 g, 0.665 mmol) in 1-propanol (40 mL) was added water (40 mL) and the resulting mixture was heated at reflux with stirring. After 6 h, the reaction mixture was cooled to room temperature and poured into water (300 mL) to form a pale yellow solid. This precipitate was collected by filtration, washed with water (50 mL), and dissolved in chloroform (100 mL). This solution was dried over Na_2SO_4, filtered, and concentrated in vacuo. Purification of the residue by flash column chromatography on silica gel (chloroform) gave **4** (0.211 g, 87%) as a pale yellow solid: IR (NaCl) 1580 cm^{-1} (C=C), 1668 cm^{-1} (C=O), 1707 cm^{-1} (C=O); ^{1}H NMR ($CDCl_3$) δ 0.80–0.93 (m, 24H, *Me*), 1.17–1.45 (m, 32H, CH_2), 1.83–1.98 (m, 4H, C*H*), 3.09 (d, *J*=6.9 Hz, 8H, CH_2), 6.30 (s, 4H, CH_2), 7.22 (d, *J*=6.7 Hz, 4H, Ar*H*), 7.39 (dd, *J*=6.7 and 8.9 Hz, 4H, Ar*H*), 8.33 (d, *J*=8.9 Hz, 4H, Ar*H*), 8.57 (s, 4H, Ar*H*), 8.87 (s, 2H, Ar*H*); ^{13}C NMR ($CDCl_3$) δ 10.4 (*C*H_3), 14.0 (*C*H_3), 23.1 (*C*H_2), 25.5 (*C*H_2), 25.6 (*C*H_2), 28.5 (*C*H_2), 32.5 (*C*H_2), 32.6 (*C*H_2), 38.4 (*C*H_2), 38.5 (*C*H_2), 38.8 (*C*H_2), 39.5 (*C*H), 121.1 (*C*H), 122.7 (*C*H), 125.6 (*C*H), 125.8 (*C*H), 126.3 (*C*), 126.4 (*C*), 128.3 (*C*), 130.0 (*C*H), 131.0 (*C*), 131.1 (*C*), 138.7 (*C*), 163.2 (*C*). Anal. Calcd for $C_{76}H_{90}N_2O_4$: C, 83.32; H, 8.28; N, 2.56. Found: C, 83.34; H, 8.08; N, 2.87.

4.2.7. 2,9-Bis(3,5-di(2-ethylhexyloxy)phenylmethyl)-2,9-diazadibenzo[cd,lm]perylene-1,3,8,10-tetraone (**5**)

A suspension of perylene-3,4,9,10-tetracarboxylic dianhydride (0.344 g, 0.877 mmol) and **3** (0.654 g, 1.80 mmol) in *N*-methyl pyrrolidinone (15 mL) was heated at 100 °C with stirring. After 10 h, the reaction mixture was cooled to room temperature and poured into water (300 mL) to form a dark red solid. This precipitate was collected by filtration, washed with water (50 mL), and dissolved in hexane (100 mL). This solution was washed with water (50 mL) and brine (30 mL), dried over Na_2SO_4, filtered, and concentrated in vacuo. Purification of the residue by flash column chromatography on silica gel (hexane/ethyl acetate=5/1) gave **4** (0.513 g, 54%) as a dark red solid: IR (NaCl) 1171 cm^{-1} (C–O), 1595 cm^{-1} (C=C), 1659 cm^{-1} (C=O), 1697 cm^{-1} (C=O); MS (MALDI-TOF) *m*/*z* 1085.1 (MH^+); HRMS (ESI) *m*/*z* calcd for $C_{70}H_{87}N_2O_8$: 1083.6462, found 1083.6514; ^{1}H NMR ($CDCl_3$) δ 0.82–0.94 (m, 24H, *Me*), 1.23–1.54 (m, 32H, CH_2), 1.61–1.74 (m, 4H, C*H*), 3.82 (d, *J*=5.6 Hz, 8H, CH_2), 5.33 (s, 4H, CH_2), 6.37 (t, *J*=2.1 Hz, 2H, Ar*H*), 6.70 (d, *J*=2.1 Hz, 4H, Ar*H*), 8.41 (d, *J*=8.0 Hz, 4H, Ar*H*), 8.58 (d, *J*=8.0 Hz, 4H, ArH); ^{13}C NMR ($CDCl_3$) δ 11.0 (*C*H_3), 13.9 (*C*H_3), 22.9 (*C*H_2), 23.7 (*C*H_2), 29.0 (*C*H_2), 30.4 (*C*H_2), 39.4 (*C*H), 70.4 (*C*H_2), 100.5 (*C*H), 107.6 (*C*H), 122.5 (*C*), 122.9 (*C*H), 125.4 (*C*), 128.6 (*C*), 131.0 (*C*H), 133.7 (*C*), 139.1 (*C*), 160.7 (*C*), 162.8 (*C*). Anal. Calcd for $C_{70}H_{86}N_2O_8$: C, 77.60; H, 8.00; N, 2.59. Found: C, 77.38; H, 7.68; N, 2.63.

4.2.8. 2,7-Bis(4,5-di(2-ethylhexyl)-9-anthracenemethyl)-1,3,6,8-tetrahydro-2,7-diazadibenzo[de,ij]naphthalene (**2**)

To a solution of aluminum chloride (0.123 g, 0.922 mmol) in anhydrous THF (7 mL) was added lithium aluminum hydride (0.035 g, 0.922 mmol) in small portions at 0 °C. After removal of the ice-bath and stirring for 30 min, **4** (0.025 g, 0.0228 mmol) was added in small portions and the reaction mixture was stirred at room temperature. After an additional 2 h, the resulting reaction mixture was quenched with water (3 mL) and 3% aqueous HCl (3 mL) at 0 °C. To the residue was added 15 wt % NaOH (5 mL) and the resulting solid was dissolved in CH_2Cl_2 (30 mL), washed with water (30 mL), and brine (30 mL). The organic layer was dried over Na_2SO_4, filtered, and concentrated in vacuo to give **2** (0.022 g, 94%) as a pale yellow solid: UV (toluene) 361 nm (ε 11,300), 378 nm (ε 19,100), 400 nm (ε 17,800); IR (NaCl) 1601 cm^{-1} (C=C), 1618 cm^{-1} (C=C), 2926 cm^{-1} (C–H), 2959 cm^{-1} (C–H), 3020 cm^{-1} (C–H); MS (MALDI-TOF) *m*/*z* 1039.1 (M^+); HRMS (ESI) *m*/*z* calcd for $C_{76}H_{99}N_2$: 1039.7808, found 1039.7883; ^{1}H NMR ($CDCl_3$) δ 0.81–0.97 (m, 24H, *Me*), 1.20–1.48 (m, 32H, CH_2), 1.85–2.05 (m, 4H, C*H*), 3.14 (d, *J*=7.2 Hz, 8H, CH_2), 4.17 (s, 8H, CH_2), 4.68 (s, 4H, CH_2), 7.03 (s, 4H, CH_2), 7.25 (d, *J*=6.7 Hz, 4H, Ar*H*), 7.35 (dd, *J*=6.7 and 8.9 Hz, 4H, Ar*H*), 8.29 (d, *J*=8.9 Hz, 4H, Ar*H*), 8.89 (s, 2H, Ar*H*); ^{13}C NMR ($CDCl_3$) δ 10.7 (*C*H_3), 14.1 (*C*H_3), 23.3 (*C*H_2), 25.9 and 26.0 (*C*H_2), 28.9 (*C*H_2), 32.9 (*C*H_2), 38.7 (*C*H_2), 39.9 (*C*H), 53.3 (*C*H_2), 56.4 (*C*H_2), 120.4 (*C*H), 122.2 (*C*H), 123.7 (*C*H), 125.5 (*C*H), 126.0 (*C*H), 128.1 (*C*), 130.4 (C), 130.8 (C), 131.9 (C), 138.6 (C). Anal. Calcd for $C_{76}H_{98}N_2$: C, 87.80; H, 9.50; N, 2.69. Found: 87.76; H, 9.19; N, 2.89.

4.2.9. 2,9-Bis(3,5-di(2-ethylhexyloxy)phenylmethyl)-1,3,8,10-tetrahydro-2,9-diazadibenzo[cd,lm]perylene (**3**)

This compound was prepared from **5** according to the procedure for preparation of **2** and obtained in 98% as bright orange-colored oil; UV (toluene) 430 nm (ε 31,000) and 458 nm (ε 41,600); IR (NaCl) 1169 cm^{-1} (C–O), 1595 cm^{-1} (C=C); MS (MALDI-TOF) *m*/*z* 1027.4

(M^+); HRMS (ESI) m/z calcd for $C_{70}H_{95}N_2O_4$: 1027.7292, found 1027.7387; ^{1}H NMR ($CDCl_3$) δ 0.85–0.95 (m, 24H, *Me*), 1.25–1.55 (m, 32H, CH_2), 1.63–1.74 (m, 4H, C*H*), 3.71 (s, 4H, CH_2), 3.81 (d, J=5.6 Hz, 8H, CH_2), 3.93 (s, 8H, CH_2), 6.41 (t, J=2.2 Hz, 2H, Ar*H*), 6.57 (d, J=2.2 Hz, 4H, Ar*H*), 7.14 (d, J=7.7 Hz, 4H, Ar*H*), 8.02 (d, J=7.7 Hz, 4H, ArH); ^{13}C NMR ($CDCl_3$) δ 11.2 (*C*H$_3$), 14.1 (*C*H$_3$), 23.1 (*C*H$_2$), 24.0 (*C*H$_2$), 29.2 (*C*H$_2$), 30.6 (*C*H$_2$), 39.6 (*C*H), 56.8 (*C*H$_2$), 62.4 (*C*H$_2$), 70.7 (*C*H$_2$), 100.5 (*C*H), 107.6 (*C*H), 119.5 (*C*H), 123.4 (*C*H), 128.5 (*C*), 129.6 (*C*), 130.3 (*C*), 133.0 (*C*), 140.5 (*C*), 160.9 (*C*). Anal. Calcd for $C_{70}H_{94}N_2O_4$: C, 81.82; H, 9.22; N, 2.73. Found: C, 81.93; H, 8.93; N, 2.60.

4.3. Typical experimental procedure for AFM analyses

The reaction mixture diluted with dry toluene (c 0.1 mM) was drop-cast on to the HOPG. Airdried sample of the reaction mixture was examined by carrying out measurements in tapping mode.

Acknowledgements

This research was supported by a Grant-in-Aid for Scientific Research and Nanotechnology Network Project (Kyushu-area Nanotechnology Network) from the Ministry of Education, Culture, Sports, Science, and Technology (MEXT), Japan.

Supplementary data

^{1}H and ^{13}C NMR spectra for all new compounds. Supplementary data associated with this article can be found in the online version, at doi:10.1016/j.tet.2009.01.089.

References and notes

1. (a) Sapsford, K. E.; Berti, L.; Medintz, I. L. *Angew. Chem., Int. Ed.* **2006**, *45*, 4562; (b) Balaban, T. S. *Acc. Chem. Res.* **2005**, *38*, 612; (c) Del Guerzo, A.; Olive, A. G. L.; Reichwagen, J.; Hopf, H.; Desvergne, J. P. *J. Am. Chem. Soc.* **2005**, *127*, 17984; (d) Röger, C.; Müller, M. G.; Lysetska, M.; Miloslavina, Y.; Holzwarth, A. R.; Würthner, F. *J. Am. Chem. Soc.* **2006**, *128*, 6542; (e) Sautter, A.; Kaletaş, B. K.; Schmid, D. G.; Dobrawa, R.; Zimine, M.; Jung, G.; van Stokkum, I. H. M.; De Cola, L.; Williams, R. M.; Würthner, F. *J. Am. Chem. Soc.* **2005**, *127*, 6719; (f) Hoeben, F. J. M.; Shklyarevskiy, I. O.; Pouderoijen, M. J.; Engelkamp, H.; Schenning, A. P. H. J.; Christianen, P. C. M.; Maan, J. C.; Meijer, E. W. *Angew. Chem., Int. Ed.* **2006**, *45*, 1232; (g) Metera, K. L.; Sleiman, H. *Macromolecules* **2007**, *40*, 3733; (h) Sugiyasu, K.; Fujita, N.; Shinkai, S. *Angew. Chem., Int. Ed.* **2004**, *43*, 1229; (i) Ajayaghosh, A.; Praveen, V. K.; Vijayakumar, C.; George, S. J. *Angew. Chem., Int. Ed.* **2007**, *46*, 6260; (j) Kelly, R. F.; Goldsmith, R. H.; Wasielewski, M. R. *J. Am. Chem. Soc.* **2007**, *129*, 6384; (k) Hajjaj, F.; Yoon, Z. S.; Yoon, M.-C.; Park, J.; Satake, A.; Kim, D.; Kobuke, Y. *J. Am. Chem. Soc.* **2006**, *128*, 4612; (l) Sagawa, T.; Fukugawa, S.; Yamada, T.; Ihara, H. *Langmuir* **2002**, *18*, 7223; (m) Sasaki, K.; Nakagawa, H.; Zhang, X.; Sakurai, S.; Kano, K.; Kuroda, Y. *Chem. Commun.* **2004**, 408; (n) Ajayaghosh, A.; Praveen, V. K.; Srinivasan, S.; Varghese, R. *Adv. Mater.* **2007**, *19*, 411.
2. (a) Vasil'ev, S.; Orth, P.; Zouni, A.; Owens, T. G.; Bruce, D. *Proc. Natl. Acad. Sci. U.S.A.* **2001**, *98*, 8602; (b) Sundström, V.; Pullerits, T.; van Grondelle, R. *J. Phys. Chem. B* **1999**, *103*, 2327; (c) McDermott, G.; Prince, S. M.; Freer, A. A.; Hawthornthwaite-Lawless, A. M.; Papiz, M. Z.; Cogdell, R. J.; Isaacs, N. W. *Nature* **1995**, *374*, 517.
3. (a) Giansante, C.; Ceroni, P.; Balzani, V.; Vögtle, F. *Angew. Chem., Int. Ed.* **2008**, *47*, 5422; (b) Adronov, A.; Fréchet, J. M. J. *Chem. Commun.* **2000**, 1701; (c) Choi, M.-S.; Yamazaki, T.; Yamazaki, I.; Aida, T. *Angew. Chem., Int. Ed.* **2004**, *43*, 150; (d) Accorsi, G.; Armaroli, N.; Eckert, J.-F.; Nierengarten, J.-F. *Tetrahedron Lett.* **2002**, *43*, 65; (e) Takahashi, M.; Morimoto, H.; Suzuki, Y.; Yamashita, M.; Kawai, H.; Sei, Y.; Yamaguchi, K. *Tetrahedron* **2006**, *62*, 3065; (f) Takahashi, M.; Morimoto, H.; Suzuki, Y.; Odagi, T.; Yamashita, M.; Kawai, H. *Tetrahedron* **2004**, *60*, 11771; (g) Takahashi, M.; Odagi, T.; Tomita, H.; Oshikawa, T.; Yamashita, M. *Tetrahedron Lett.* **2003**, *44*, 2455; (h) Chrisstoffels, L. A. J.; Adronov, A.; Fréchet, J. M. J. *Angew. Chem., Int. Ed.* **2000**, *39*, 2163; (i) Beckers, E. H. A.; van Hal, P. A.; Schenning, A. P. H. J.; El-ghayoury, A.; Peeters, E.; Rispens, M. T.; Hummelen, J. C.; Meijer, E. W.; Janssen, R. A. J. *J. Mater. Chem.* **2002**, *12*, 2054; (j) Nakashima, T.; Kimizuka, N. *Adv. Mater.* **2002**, *14*, 1113; (k) Cabanillas-Gonzalez, J.; Fox, A. M.; Hill, J.; Bradley, D. D. C. *Chem. Mater.* **2004**, *16*, 4705; (l) Wolak, M. A.; Melinger, J. S.; Lane, P. A.; Palilis, L. C.; Landis, C. A.; Delcamp, J.; Anthony, J. E.; Kafafi, Z. H. *J. Phys. Chem. B* **2006**, *110*, 7928; (m) Ajayaghosh, A.; Praveen, V. K.; Vijayakumar, C. *Chem. Soc. Rev.* **2008**, *37*, 109; (n) Praveen, V. K.; George, S. J.; Varghese, R.; Vijayakumar, C.; Ajayaghosh, A. *J. Am. Chem. Soc.* **2006**, *128*, 7542; (o) Ajayaghosh, A.; Vijayakumar, C.; Praveen, V. K.; Babu, S. S.; Varghese, R. *J. Am. Chem. Soc.* **2006**, *128*, 7174; (p) Ajayaghosh, A.; George, S. J.; Praveen, V. K. *Angew. Chem., Int. Ed.* **2003**, *42*, 332.
4. (a) Mondal, S. K.; Ghosh, S.; Sahu, K.; Mandal, U.; Bhattacharyya, K. *J. Chem. Phys.* **2006**, *125*, 224710; (b) Cringus, D.; Bakulin, A.; Lindner, J.; Vöhringer, P.; Pshenichnikov, M. S.; Wiersma, D. A. *J. Phys. Chem. B* **2007**, *111*, 14193; (c) Ryu, J.-H.; Lee, M. *J. Am. Chem. Soc.* **2005**, *127*, 14170; (d) Chen, C.-Y.; Tian, Y.; Cheng, Y.-J.; Young, A. C.; Ka, J.-W.; Jen, A. K.-Y. *J. Am. Chem. Soc.* **2007**, *129*, 7220.
5. Takahashi, M.; Ichihashi, Y.; Nishizawa, N.; Ohno, S.; Fujita, N.; Yamashita, M.; Sengoku, T.; Yoda, H. *J. Photochem. Photobiol. A: Chem.*, in press. doi:10.1016/j.jphotochem.2008.12.022
6. Melhuish, W. H. *J. Phys. Chem.* **1963**, *67*, 1681.
7. (a) Würthner, F.; Sautter, A.; Thalacker, C. *Angew. Chem., Int. Ed.* **2001**, *39*, 1243; (b) Takahashi, M.; Suzuki, Y.; Ichihashi, Y.; Yamashita, M.; Kawai, H. *Tetrahedron Lett.* **2007**, *48*, 357.
8. In our previous study employing **1**, we demonstrated that the reverse micelles should have a uniform aggregate size independent of the W_0 value. For this reason, we used the W_0 value of 50 as a representative self-assembly condition.
9. We previously demonstrated that nanoscopic-sized reverse micelles preparaed from the related analogue **1** achieved either efficient intramolecular energy transfer or collisional dissipation due to intermolecular chromophore interactions.
10. Possibilities of energy transfer between the self-assembled aggregates can be ruled out on the basis of the experimental conditions employing sufficiently dilute solutions of the analytes.
11. (a) Takahashi, M.; Morimoto, H.; Miyake, K.; Kawai, H.; Sei, Y.; Yamaguchi, K.; Yamashita, M.; Sengokua, T.; Yoda, H. *New J. Chem.* **2008**, *32*, 547; (b) Takahashi, M.; Morimoto, H.; Miyake, K.; Yamashita, M.; Kawai, H.; Sei, Y.; Yamaguchi, K. *Chem. Commun.* **2006**, 3084; (c) Takahashi, M.; Morimoto, H.; Suzuki, Y.; Yamashita, M.; Kawai, H. *Polym. Prepr. (Am. Chem. Soc., Div. Polym. Chem.).* **2004**, *45*, 959.
12. In order to gain further insight into the mechanism of the energy transfer processes, fluorescence lifetime studies on the reverse micelles are needed. However, our attempts to obtain the fluorescence lifetime data (τ) failed due to limited time resolution of the experimental setup.
13. Application of the Stern–Volmer plots yielded the Stern–Volmer constant K_{SV} (1.2×10^4 M^{-1}) for the series of the mixed reverse micelles. Thus, the rate constant of energy transfer k_{ET} (3.1×10^{11} M^{-1} s^{-1}) was estimated using the reported fluorescence lifetimes τ (1.4 ns (14%), 4.3 ns (23%) and 60.5 ns (63%)) of the anthracene aggregate system in micelles, which was closely related to the donor-based reverse micelles prepared from **2**. As for this anthracene aggregate system, see: Chen, K.-H.; Yang, J.-S.; Hwang, C.-Y.; Fang, J.-M. *Org. Lett.* **2008**, *10*, 4401.
14. For further details and some theoretical bases for the Förster process, see: the relative ratio of the peaks corresponding to the anthracene donor, while normalizing for the peaks corresponding to the perylene acceptor, can be used to estimate the energy transfer efficiency. According to this methodology, the energy transfer efficiencies were estimated to be 0.71, 0.77, and almost quantitative for the reverse micelles at the feed ratios (**2**/**3**) of 95/5, 91/9, and the other members of the series (i.e., **2**/**3**=83/17, 75/25, 67/33, 50/50, 33/67, 25/75, 17/83, 9/91, and 5/95), respectively Valeur, B. *Molecular Fluorescence Principles and Applications*; Wiley-VCH: Weinheim, New York, Chichester, Brisbane, Singapore, Toronto, 2002; Chapter 9, pp 247–272.
15. In our previous study employing **1**, we reproducibly obtained small-sized spherical objects when the solutions at different concentrations in toluene were cast on the HOPG substrates. Based on those reproducible observations, we concluded that the small-sized peaks could be attributed to the individual reverse micelles and thus the medium-sized peaks should correspond to their assemblies.
16. For aggregate size determination, dynamic light scattering (DLS) measurements have been performed on the reverse micelles. However, attempts to record particle size distributions failed due to experimental limitations of the setup.
17. At highly dilute concentrations of the surfactants below the cmc, where the surfactants gathering in the reverse micellar forms should become dissociated, the fluorescence spectra of the samples were identical to that of the monomeric perylene emission, whose intensity should increase linearly with the solute concentrations. On the other hand, the formation of the reverse micelles leads to introduction of the radiationless deactivation channels due to the chromophore clustering, resulting in nonlinear dependency of the fluorescence intensities on the solute concentrations. For these reasons, we considered that titration experiments performed by monitoring the intensity of the fluorescence emission from the chromophoric components allowed precise evaluation of the cmc values. As for similar procedures for cmc estimations, see: (a) Goodwin, A. P.; Mynar, J. L.; Ma, Y.; Fleming, G. R.; Fréchet, J. M. J. *J. Am. Chem. Soc.* **2005**, *127*, 9952; (b) Jung, C.; Müller, B. K.; Lamb, D. C.; Nolde, F.; Müllen, K.; Bräuchle, C. *J. Am. Chem. Soc.* **2006**, *128*, 5283; (c) Kang, L.; Wang, Z.; Cao, Z.; Ma, Y.; Fu, H.; Yao, J. *J. Am. Chem. Soc.* **2007**, *129*, 7305; (d) Sutthasupa, S.; Sanda, F.; Masuda, T. *Macromolecules* **2008**, *41*, 305.
18. (a) Xu, S.; Giuseppone, N. *J. Am. Chem. Soc.* **2008**, *130*, 1826; (b) Ma, Y.; Kolotuchin, S. V.; Zimmerman, S. C. *J. Am. Chem. Soc.* **2002**, *124*, 13757.
19. (a) Wang, B.-B.; Gao, M.; Jia, X.-R.; Li, W.-S.; Jiang, L.; Wei, Y. *J. Colloid Interface Sci.* **2008**, *324*, 225; (b) Beckers, E. H. A.; Jonkheijm, P.; Schenning, A. P. H. J.; Meskers, S. C. J.; Janssen, R. A. J. *ChemPhysChem* **2005**, *6*, 2029.